

# Parvoviral Infection of Endothelial Cells and Its Possible Role in Vasculitis and Autoimmune Diseases

CYNTHIA M. MAGRO, A. NEIL CROWSON, MAGDY DAWOOD, and GERARD J. NUOVO

**ABSTRACT. Objective.** To analyze a series of biopsies from 16 patients who, on the basis of clinical and dermatopathologic findings, had a spectrum of connective tissue diseases (CTD), autoinflammatory or CTD-like syndromes for parvoviral DNA, RNA, and protein.

**Methods.** Most of the patients were initially screened for parvoviral-related IgG and IgM antibodies. Parvoviral DNA was analyzed by solution phase polymerase chain reaction (PCR). *In situ* localization of viral VP1 RNA was accomplished by *in situ* reverse transcriptase (RT) PCR; viral protein (VP2) was detected by immunohistochemistry and these results correlated with the histologic findings. (J Rheumatol 2002;29:xxxx)

**Results.** Of 11 people tested, 10 had either IgG or IgM specific antibodies against parvovirus. Common histologic features of the 16 cases included an interface dermatitis, interstitial histiocytic infiltration with variable collagen necrobiosis, a mononuclear cell dominant vasculitis, and interstitial neutrophilia. Detection of parvoviral RNA by *in situ* RT-PCR in 14 of 16 cases corroborated solution phase PCR data and demonstrated that the endothelial cells and surrounding mononuclear cells were the viral target. Viral protein as revealed by immunohistochemistry showed an equivalent histologic distribution. Anti-tumor necrosis factor- $\alpha$  (TNF- $\alpha$ ) therapy (etanercept) yielded dramatic improvement after worsening of symptoms with traditional immunosuppressive therapy in the 3 patients in whom this drug was administered; TNF- $\alpha$  mRNA was detected by *in situ* RT-PCR in the area of parvoviral infected cells.

**Conclusion.** Parvoviral induced endothelialitis may be responsible for cases of "idiopathic" CTD. (J Rheumatol 2002;29:1227-35)

## Key Indexing Terms:

PARVOVIRUS  
CONNECTIVE TISSUE DISEASE

B19

VASCULITIS  
AUTOIMMUNE DISEASE

Viral infections have long been postulated as an inciting factor in autoimmune connective tissue diseases (CTD) as well as vasculitides polyarteritis nodosa (PAN), mixed cryoglobulinemia, Kawasaki's disease, and Wegener's granulomatosis (WG). The prototypic virally mediated vasculitic syndrome is hepatitis C associated mixed cryoglobulinemia<sup>1</sup>, where persistent viral infection is speculated to induce formation of autoantibodies. Other viruses potentially involved in CTD include Epstein-Barr virus and parvovirus B19 (B19), varicella zoster, and cytomegalovirus<sup>2,3</sup>. B19, the etiologic agent of the common childhood exanthem fifth disease, has recently been implicated in autoimmune diseases and CTD in children and adults

including WG<sup>4,5</sup>, Henoch Schönlein purpura (HSP)<sup>6</sup>, Kawasaki disease<sup>7</sup>, and temporal arteritis<sup>8</sup>. Most of these studies have implicated B19 through serological documentation of acute and/or chronic persistent infection<sup>6-8</sup>. Although B19 DNA has recently been documented by solution phase polymerase chain reaction (PCR) in skin biopsies from patients with CTD<sup>9</sup>, to our knowledge direct *in situ* localization of B19 nucleic acids or antigens has not been documented.

The vast majority of CTD syndromes have a cutaneous expression, which may be the first clinical sign of a multi-organ disease process. The classic clinical cutaneous presentations encompass photodistributed papulosquamous and erythematous eruptions, nodules and annular plaques often with localization to the joint surfaces, periungual erythema, and vasculitic lesions, the latter manifested by palpable purpura, livedo, and ulceration. The histologic appearance is one of interface dermatitis and/or perivascular inflammation. Other histologic findings include an interstitial histiocytic infiltration with variable collagen necrobiosis, paucinflamatory thrombosis, a mononuclear cell or neutrophilic vasculitis, interstitial neutrophilia, and dermal mucin. These histologic features, although consistent with chronic antigenic stimulation, do not in themselves suggest a specific etiology. Direct viral localization in CTD is not

From the Department of Pathology, Ohio State University, Columbus, OH, USA; Central Medical Laboratories, Winnipeg, MB, Canada; Regional Medical Laboratories, Tulsa, OK, USA; Cadham Provincial Laboratories, Winnipeg.

Supported by Grant AN3042-GJN from the Lewis Foundation.

C.M. Magro, MD, Professor of Pathology, Ohio State University;  
A.N. Crowson, MD, Associate Professor of Dermatology, Central Medical Laboratories; M. Dawood, PhD, Cadham Provincial Laboratories;  
G.J. Nuovo, MD, Professor of Pathology, Ohio State University.

Address reprint requests to Dr. G.J. Nuovo, Department of Pathology, Ohio State University, S305 Rhodes Hall, 450 W 10th Avenue, Columbus, Ohio 43210. E-mail: gnuovomd@pol.net

Submitted July 18, 2001; revision accepted November 8, 2001.

well documented. One exception is that HIV-1 spliced transcripts have been detected *in situ* in macrophages in the dermatomyositis-like syndrome of AIDS (so called AIDS myopathy)<sup>10</sup>.

We present clinical and histological findings similar to the aforesaid prototypic cutaneous presentation of CTD or autoinflammatory conditions in 16 patients whereby the integrated clinical, light microscopic, immunohistochemical, and molecular profile implicated a causal role of B19 infection in 14 of these people.

## MATERIALS AND METHODS

**Selection of cases.** The selection criteria for this study were that the clinical and histologic information was consistent with cutaneous manifestation of CTD, autoinflammatory conditions and/or vasculitis. A characteristic clinical feature was that the symptomatology was unresponsive to standard immunosuppressive therapy. The light microscopic criteria were a mononuclear cell dominant vascular injury process associated with interface dermatitis, and foci of diffuse interstitial granulomatous inflammation or neutrophilia. Sixteen cases met these clinical and histologic criteria. Serology was available in 11 of the cases and in 10 indicated prior infection with B19.

**Immunofluorescent studies.** Skin biopsy material received in Michel's transport medium and subsequently stored at  $-30^{\circ}\text{C}$  was available in 4 cases. Direct immunofluorescence studies for IgG, IgA, IgM, fibrin, and C3 (DAKO, Dimension Laboratories, Mississauga, Ontario, Canada) were performed on lesional skin by the overlay of fluorescein-conjugated antibody upon sections cut from frozen skin and examined using a fluorescent microscope. An indirect immunofluorescence methodology with a fluorescein-conjugated rabbit anti-mouse antibody was used to detect the presence of C<sub>5b,9</sub> in frozen sections in 2 of the cases.

**Molecular studies.** DNA was extracted from both paraffin embedded and frozen skin biopsies. The DNA was extracted from the paraffin embedded tissues according to previously published methods<sup>11</sup>. Nested PCR for B19 DNA was carried out by the method of Fridell, *et al*<sup>11</sup>. The first set of primers amplified a 405 bp segment on the parvovirus B19 genome and the second set of primers amplified a 286 bp amplicon. Two negative control samples (reagent control and DNA from a known B19 seronegative individual) and 3 positive controls (10 and 100 copies of the pYT104-C recombinant plasmid containing B19 genome) as well as a known B19 positive serum sample were included in each run. Twenty microliters of the PCR products were analyzed on a 3% agarose gel after electrophoresis. The gels were stained with ethidium bromide, DNA bands were visualized using UV light, and the presence of a 286 bp band was taken as an indication of a positive specimen. A series of negative control specimens were run comprising biopsy specimens from the following: sclerosing basal cell carcinoma, a lesion of diabetes associated granuloma annulare, an angiokeratoma, a carbon tattoo, stasis dermatitis, molluscum contagiosum, and a melanocytic nevus.

**In situ reverse transcriptase (RT)-PCR.** The protocol used in this study for paraffin embedded, formalin fixed tissues has been described<sup>12,13</sup>. Optimal protease digestion time was first determined using as the guide nonspecific incorporation of the reporter nucleotide. Optimal protease digestion was followed by overnight incubation in RNase free-DNase (10  $\mu\text{m}$  per sample, Boehringer Mannheim, Indianapolis, IN, USA) and one step RT-PCR using the rTth system and digoxigenin dUTP as described<sup>12,13</sup>. The tissue was analyzed for parvoviral RNA using a primer sequence for the VP1 region, indicative of a productive infection, as described<sup>12</sup>. After 25 cycles, the digoxigenin labeled cDNA was detected due to the action of alkaline phosphatase on the chromogen nitroblue tetrazolium and bromochloroindolyl phosphate. Nuclear fast red served as the counterstain. Biopsy material from lesions manifesting comparable light microscopic findings including

necrotizing vasculitis, pauciinflammatory thrombosis, necrotizing folliculitis, palisading granulomatous inflammation, and interface dermatitis in which the basis of the eruption was known and not attributed to B19 were used as negative controls. A total of 18 negative controls were run (12 from the first group matched according to reaction patterns encountered in B19 infection) and 6 from miscellaneous lesions that served as the negative controls for the solution PCR assay (see above). The tissue samples were also examined for evidence of tumor necrosis factor- $\alpha$  (TNF- $\alpha$ ) mRNA expression using *in situ* RT-PCR as described<sup>13</sup> to determine if this cytokine was upregulated in the case samples.

**Immunohistochemistry.** Our protocol for paraffin embedded, formalin fixed tissues has been described<sup>12</sup>. Detection using the parvoviral specific antibody (DAKO) directed against the VP2 structural protein was optimized at a dilution of 1:50 and with a pretreatment of proteinase K (100  $\mu\text{g}/\text{ml}$ ) for 10 min using a case of parvoviral placentitis.

## RESULTS

**Clinical information.** A summary of the clinical information about the patients included in this study is provided in Table 1. Patients ranged in age from 17 to 76 years; there were 11 women and 5 men. In 4 patients (cases 1, 5-7) lesional onset was temporally associated with exposure to fifth disease. Thirteen of the patients showed evidence of a systemic CTD syndrome including fatigue, arthritis, and myalgias. American College of Rheumatology criteria were fulfilled for rheumatoid arthritis (RA) (1 patient), microscopic PAN (1 patient), HSP (2 patients), and mixed connective tissue disease (1 patient). In 4 patients hybrid presentations comprising heliotropes, periungual erythema and/or Gottron's papules, hence resembling dermatomyositis in concert with malar erythema or other lupus-like rashes, lesions resembling rheumatoid papules on digits and symmetrical small joint arthritis were observed (Figure 1). A primary vasculitic syndrome was seen in 7 patients that in 2 patients was compatible with IgA vasculitis/HSP and in one patient with perinuclear antineutrophil cytoplasmic antibody (ANCA) positive microscopic PAN; in the remaining patients the vasculitis was largely confined to the skin. Two patients had an autoinflammatory symptom complex resembling familial Mediterranean fever as characterized by recurrent erysipeloid erythema (Figure 1) accompanied by fever and arthralgias. A concomitant anterior thigh rash was also evident in most patients independent of other aspects of the clinical presentation (Figure 1). Many of the patients had a personal or family history of atopy comprising asthma, eczema, and allergic rhinitis. In 3 of the cases (case 6, 7, 12) spontaneous remission occurred within weeks of onset of illness. Ten of the 11 cases where serology was available evidenced recent B19 exposure, documented by markedly elevated IgG levels; 4 patients also had concomitant IgM antibody positivity including 2 who had spontaneous resolution of symptoms. In the people with persistent symptomatology, standard immunosuppressive therapy had not been effective. Finally, the 3 patients receiving anti-TNF therapy (subcutaneous doses of 25 mg twice weekly of etanercept) experienced a rapid and dramatic improvement of

Table 1. Clinical manifestations of patients with vasculitis/connective tissue disease syndromes.

Case	Age/Sex	CTD Syndrome	Skin Manifestations	Extracutaneous Manifestations	B19 and Other Serology	Therapy	Duration and Outcome
1	27 F	RA/SLE/DM overlap	Violaceous heliotrope; symmetrical malar plaques; SCLÉ-like annular papulosquamous rash arm, chest & back; rheumatoid like papules and nodules over fingers and elbows	Arthritis; fatigue; myalgias	B19 IgG	Prednisone, etanercept, methotrexate, nabumetone	1.5 yrs; marked improvement with etanercept
2	45 M	Folliculocentric vasculitis	Follicular-based purpura	Fatigue and arthritis; ↑ liver function tests	B19 IgG, cryoglobulinemia	Azathioprine, pentoxifylline, Thalidomide, Colchicine, α-interferon, γ-globulin, prednisone; etanercept	3 yrs; marked improvement with etanercept
3	62 F	Microscopic PAN	Pustular vasculitis	Conjunctivitis, polyarthritis, hemoptysis, GN	B19 IgG, ANA (1:2024) + pANCA	Cyclophosphamide	1 yr; renal disease persists
4	17F	MCTD	Erythematous scaly rash on thighs	Myositis, arthritis	B19 IgG, ANA (1:1280), anti-RNP (1:512)	Prednisone; hydroxychloroquine	1 yr; myositis, arthritis, rash persist
5	46 F	Chilblains lupus-like with overlap features of DM	Violaceous acral papules; periungual erythema, petechial hemorrhages of finger tips	Fatigue, arthralgia	B19 IgG	Nonsteroidal anti-inflammatory agents	10 mo; rash, fatigue, myalgias persist
6	45 F	Lymphocytic vasculitis	Brick red confluent rash over both lower extremities with sparing of feet	Fatigue, malaise, arthritis	B 19 IgG and IgM	None	Resolved in 1 week
7	39 F	Lymphocytic vasculitis	Petechial eruption over the extremities	None	B19 IgG and IgM	None	Resolved in 2 weeks
8	73 F	Undefined	Generalized annular lesions	Fatigue, myalgias arthralgias	B19 negative	Prednisone	Persists after 3 yrs
9	53 F	Undefined	Erysipeloid urticarial-like erythema	Malaise, fever	NA	Prednisone	Persists after 1 yr
10	60 M	IgA mediated vasculitis	Palpable purpura of legs, thighs, lower trunk	Arthralgias	B19 IgG and IgM	No treatment	Resolved with no complications
11	76 M	IgA based LCV	Palpable purpura	Arthralgias	NA	Prednisone	Persists at 6 mo
12	34 M	SLE-like illness with DM	Infiltrative erythema face, periorbital discoloration	Fatigue and arthralgias	B19 IgG, ANA	No therapy	Resolved after 6 weeks
13	72 F	Gr vasculitis/ palisading granulomas presenting with DM	DM-like heliotrope, Gottron's like papules, infiltrative plaques back and extremities	Symmetrical polyarthritis	High B19 IgM	Etanercept	Marked improvement with etanercept
14	72 M	Gr vasculitis/ granuloma	Violaceous plaques on hands	None	NA	No therapy	Persists
15	36 F	Sweet's-like syndrome	Erysipeloid erythema on thigh	Malaise and periodic fever	NA	Prednisone	Persists
16	46 F	Undefined	Blisters distal phalynx of left 5 <sup>th</sup> digit	None	NA	Prednisone	Recurred, then spontaneously resolved

ANA: antinuclear antibody; CTD: connective tissue disease; DM: dermatomyositis/DMSM–DM sine myositis; PAN: polyarteritis nodosa; SLE: systemic lupus erythematosus; GMN: necrotizing crescentic glomerulonephritis; RNP: ribonuclear protein; Gr: granulomatous; MCTD: mixed connective tissue disease; pANCA: perinuclear antineutrophil cytoplasmic antibody; RA: rheumatoid arthritis; LCV: leukocytoclastic vasculitis; SCLÉ: subacute cutaneous lupus erythematosus; NA: Not available.

symptoms despite having failed to respond to standard immunosuppressive therapy.

**Histopathology.** Skin biopsies in most cases revealed lymphocytic vacuolar interface dermatitis with or without eczematous epithelial changes. Nine of the 16 biopsies showed focal interstitial histiocytic infiltrates reminiscent of

a granuloma annulare tissue reaction. In 2 cases, foci of palisading histiocytes surrounding areas of complete collagen necrobiosis with mesenchymal mucin deposition were evident (Figure 2). A mononuclear cell dominant vasculitis of varying severity was identified in 15 of the cases (Figure 2). The vasculitis had a frankly granulomatous



*Figure 1.* Clinical features of the cutaneous manifestation of parvoviral infection. A. Bilateral violaceous heliotrope clinically held to be diagnostic of dermatomyositis (case 13, Table 1). B. Urticarial-like erythema over the abdomen accompanied by fever and arthralgias, unresponsive to prednisone (case 9). C. Violaceous erythema over the metacarpophalangeal joints compatible with Gottron's sign along with periungual erythema (case 13). D. Example of the erythematous plaques (case 13); the presence of an anterior thigh rash in concert with other cutaneous features typical of connective tissue disease was evident in several patients. Violaceous papules on the digits reminiscent of a rheumatoid papule (case 1) are shown in E.

morphology in 4 of the biopsies.

Additional morphologic patterns were seen in several cases. Extensive feulgen positive basophilic debris was identified in 3 cases, consistent with marked cell degeneration (Figure 2). Prominent extravascular neutrophilia was observed in 5 cases including in the context of intraepithelial pustulation that in one case was folliculocentric. A leukocytoclastic vasculitis was identified in 2 cases. In case

4 and 10 representing a patient with mixed collagen vascular disease and HSP, respectively, the dominant vascular reaction pattern was a pauciinflammatory vasculopathy with conspicuous endothelial cell detachment and necrosis. Biopsies in cases 9 and 15 also showed a Sweet's-like vascular reaction comprising a mixed mononuclear and neutrophilic perivascular infiltrate unaccompanied by mural or luminal fibrin deposition.

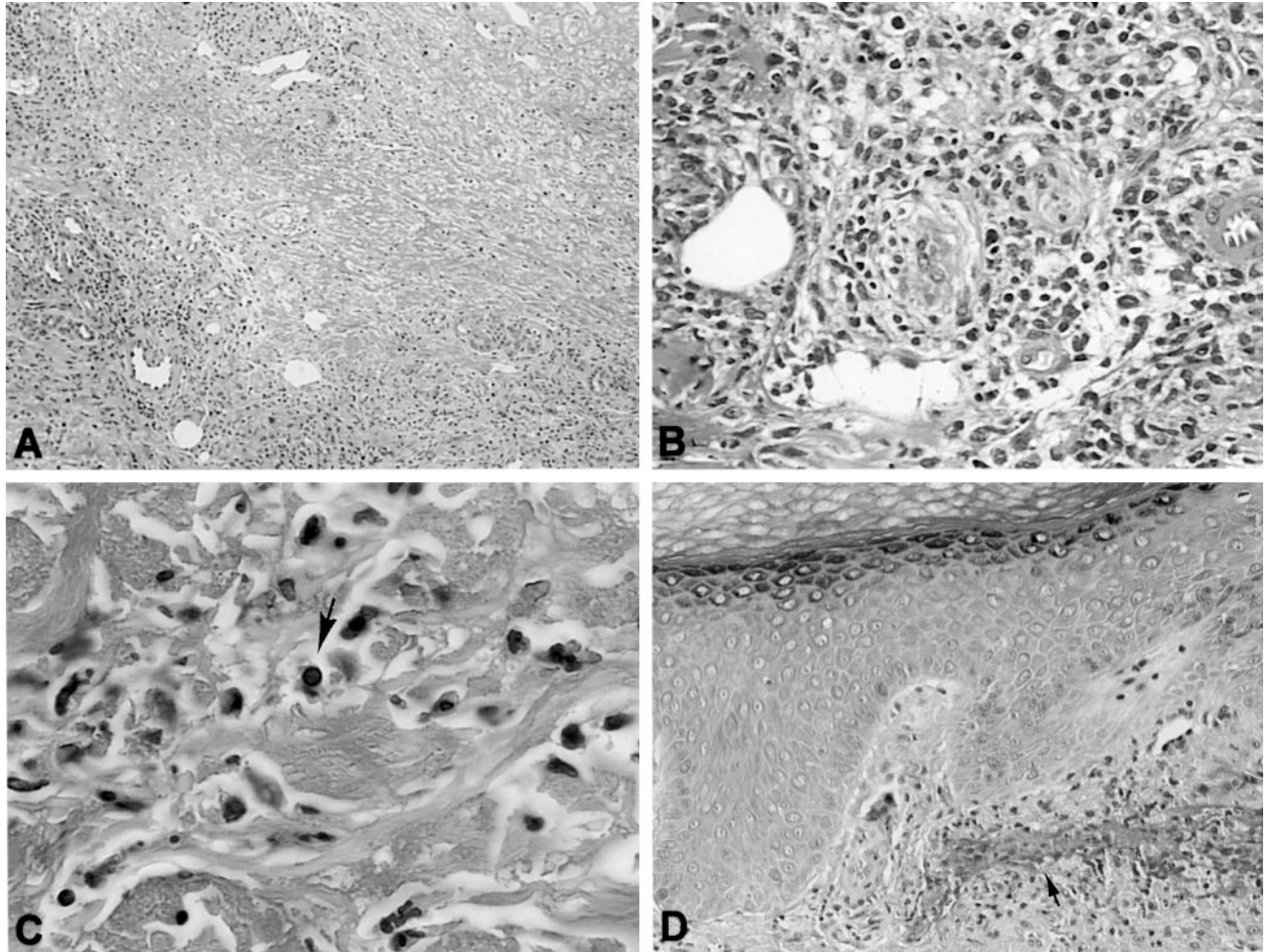


**Figure 2.** Histologic features of the cutaneous manifestation of parvoviral infection. The biopsy from case 13 is remarkable for a mononuclear cell dominant vasculitis with concomitant infiltration of the interstitium by histiocytes (A and, at higher magnification, B). Note foci of palisading granulomatous inflammation around hypereosinophilic necrobiotic collagen. Cytopathic changes attributed to B19 are present as characterized by cells showing round nuclei with an effaced chromatin and a markedly condensed rim of chromatin around the nucleus (arrow, C). D. Papillary dermis edema and associated basophilic debris (arrow).

In several of the cases B19 associated cytopathic changes were observed in occasional endothelial cells. The cells exhibited eosinophilic to amphophilic smudged nuclei with effaced chromatin (Figure 2). The nuclear membranes were unusually thickened and showed variable disruption. The cytoplasm was homogeneous eosinophilic to gray or amphophilic in quality. Eosinophilic intranuclear inclusions were present in some cells. The cells were most conspicuous in zones of basophilic body formation.

**Immunofluorescence.** Immunofluorescence testing was carried out in 6 cases. Antinuclear antibodies (ANA), anti-dsDNA antibodies, and antibodies to extractable nuclear antigens Smith (Sm), SSA/Ro, SSB/La, and ribonucleoprotein (RNP) and ANCA were sought. The cases showed a direct immunofluorescence pattern compatible with a vascular injury syndrome with localization of C<sub>5b-9</sub> to the cutaneous vasculature. No case showed a positive lupus band test or

decoration of the nuclei or cytoplasm of epidermal keratinocytes for IgG or C<sub>5b-9</sub>. In case 11 there was prominent deposition of IgA within the cutaneous vasculature.

**Solution phase PCR.** Solution phase PCR was first used to determine if B19 DNA could be detected in the tissue samples. Tissue was available in 13 cases; in 8 of these parvoviral DNA was detected. The controls listed in Materials and Methods gave the expected negative results. The PCR positive cases could represent circulating viral DNA unrelated to the histologic changes and PCR negative cases could represent relatively poor sensitivity as we have reported in paraffin embedded tissue samples<sup>13</sup>.

**In situ RT-PCR.** To further address the issue of the significance of B19 detection and determine the target cell(s) of infection, *in situ* RT-PCR was done using primers specific for the VP1 message. Fourteen of the 16 cases (88%) were positive. One of the cases negative for B19 RNA (case 2)

was positive by serology and solution phase PCR. Interestingly, this tissue did demonstrate hepatitis C mRNA in the skin lesion by *in situ* hybridization analysis (data not shown). The other negative case was case 8, which also had negative serology. The signal in the 14 positive cases localized primarily to the vascular endothelium with variable expression in surrounding mononuclear cells (Figure 3). Co-labeling experiments showed that most of the perivascular viral infected cells co-localized with CD45 while the infected cells lining small blood vessels did not co-label with CD45 but rather with factor VIII (data not shown). The number of positive cells ranged from 1+ (from 1 to 10) in 2 cases, to 2+ (11–20) in 3 cases, and 3+ (greater than 21) in the other 9 cases. Endothelial cells not associated with inflammation were usually parvovirus negative, implying that the perivascular inflammation was in response to viral endothelial cell parasitism. The positive control (B19 infected placenta) showed viral detection restricted to cells with the typical nuclear inclusions (Figure 3). All negative controls, including cases with equivalent histologic findings (i.e., mononuclear cell dominant vasculitis with necrobiosis, leukocytoclastic vasculitis, palisading granulomatous inflammation, pauciinflammatory thrombosis, interface dermatitis, and folliculitis, where a specific non parvoviral etiology had been demonstrated), were negative for B19 RNA by *in situ* RT-PCR (data not shown). Finally, the signal in the B19-infected tissues was eliminated by pretreatment in RNase, demonstrating that it was RNA-based (Figure 3).

To provide additional evidence on the specificity of the *in situ* RT-PCR results, and to demonstrate productive viral infection, immunohistochemistry was done on serial sections to those used for *in situ* RT-PCR. Viral protein was detected in 11/16 cases, including all cases positive by *in situ* RT-PCR. An equivalent histologic distribution was demonstrated, with signal localization mainly to endothelial cells in areas of inflammatory infiltrates (Figure 3). The number of positive cells was in general less than *in situ* RT-PCR (most cases were 1+ or 2+), perhaps reflecting the greater sensitivity of the *in situ* RT-PCR assay.

Since the 3 cases in which etanercept was used showed striking response to treatment, we next analyzed TNF- $\alpha$  expression by *in situ* RT-PCR in serial sections to those in which viral RNA was detected. An equivalent distribution of TNF- $\alpha$  mRNA was detected; the positive cells were primarily endothelial cells and the neighboring mononuclear cells in the same cell groups in which viral RNA and protein were detected (Figure 3). There was approximately a 1:1 ratio of cells expressing TNF- $\alpha$  to those infected by parvovirus.

## DISCUSSION

A variety of chronic diseases marked by vasculitis have been associated with serological evidence of parvovirus infection. For example, Kawasaki's disease is reported in children in whom parvovirus specific antibodies and DNA

in the peripheral blood have been identified<sup>6</sup>. Small vessel vasculitic syndromes associated with parvovirus infection include cases of pediatric WG and microscopic PAN<sup>4,5,14,15</sup>, where B19 DNA has been isolated from the peripheral blood and skeletal muscle. Such cases have shown poor response to cyclophosphamide and other immunosuppressive agents, which are standard therapy in such cases. The other small vasculitic syndrome associated with serologic evidence of recent parvovirus infection is HSP<sup>16,17</sup>. Recent reports associate larger vessel vasculitic syndromes with B19 infection. One study found an association between histologic evidence of giant cell arteritis and the presence of parvovirus DNA in tissue<sup>18</sup>. However, serologic evidence of B19 infection in such cases is circumstantial as antibodies can persist long after the end of any clinical symptoms in the self-limited form of viral disease<sup>19</sup>. None of the studies document *in situ* localization of the virus correlated to the histopathology. We present 16 patients whose clinical presentations resembled and/or fulfilled criteria for select CTD and autoinflammatory conditions. While 3 cases had a short self-limited course associated with acute viral serology, the clinical presentations in the remainder have followed a refractory course of months to years, indicative of chronic persistent disease. Direct infection of endothelial cells and neighboring mononuclear cells by parvovirus was documented by *in situ* RT-PCR in 14 of the cases; immunohistochemistry for viral antigens showed an equivalent histologic distribution. Although speculative, it is possible that the pathophysiology in part was related to TNF- $\alpha$ , as evidenced by the increased expression of the cytokine in the areas with infected cells and dramatic resolution of symptoms immediately upon treatment with etanercept in each person so treated. However, this will require further study as there were only 3 etanercept treated patients available to us for study.

As would be expected in CTD and autoinflammatory disorders, the symptom complexes were protean. Three of the patients had a hybrid cutaneous eruption comprising a striking dermatomyositis-like heliotrope or Gottron-like papules and periungual erythema; however, generalized infiltrative plaques on the extremities and trunk unassociated with classic dermatomyositis were observed in all three. Further at variance with classic dermatomyositis was the presence of a symmetrical nonerosive polyarthritides. Five patients had lesions of classic palpable purpura, in one of whom criteria for a diagnosis of microscopic PAN were fulfilled, and in two of whom vascular IgA deposition was observed, a finding compatible with HSP. The remaining 5 patients had folliculocentric vasculitis, which is recently described in association with various etiologies including virally mediated CTD<sup>20</sup>, accompanied by arthralgias (1), mixed connective tissue disease (1), generalized granuloma annulare with nonerosive arthritis (1), a systemic lupus erythematosus-like illness (1), and recurrent abdominal urticaria accompanied by arthritis and fever (1).

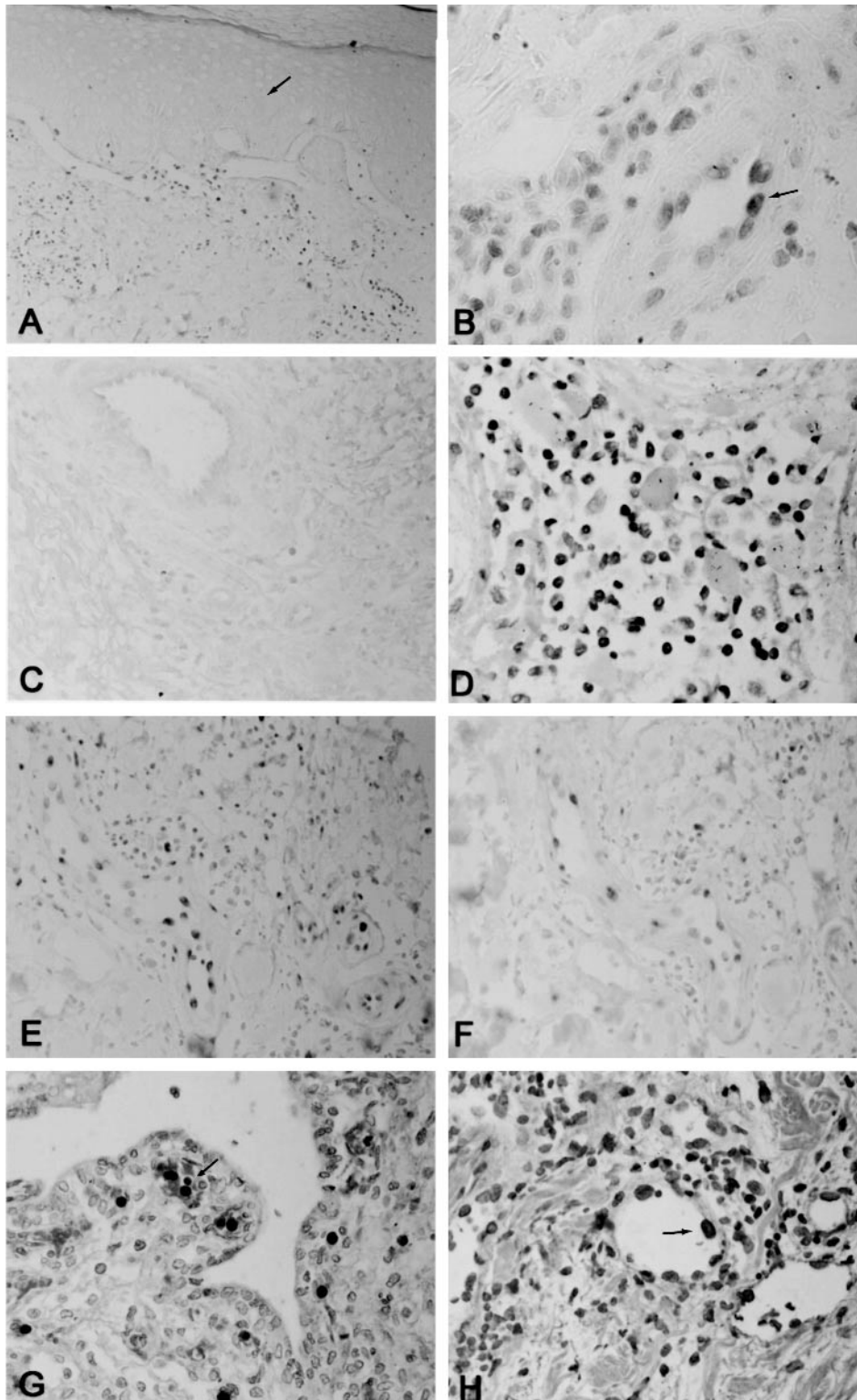


**Figure 3.** Molecular detection of parvovirus in the skin. A. Detection of parvoviral RNA (dark area is positive due to NBT/BCIP — nuclear fast red counterstain) by *in situ* RT-PCR. Note the perivascular distribution, the large number of infected cells, and the absence of a signal in the overlying epithelium (arrow). At higher magnification, note the infected endothelial cells (arrow) and surrounding mononuclear cells (case 13). The signal was lost if the section was pretreated with RNase, demonstrating that it is RNA based (C). TNF- $\alpha$  expression was also documented in a similar distribution (D). E, F. Serial section analyses of B19 (E) and TNF- $\alpha$  detection, showing the equivalent geographic distribution of the two cDNA. G. Detection of B19 protein in the nucleated red blood cells of an infected placenta (arrow, dark body is positive due to DAB, hematoxylin counterstain) and not the surrounding trophoblasts or Hofbauer cells. B19 protein was also detected in the endothelial cells (arrow) and surrounding mononuclear cells in an identical distribution to the PCR amplified cDNA (H, case 13).

While the clinical presentations were somewhat heterogeneous, the pathology in all cases demonstrated striking vasculopathic changes suggesting that vasculopathy was integral to lesional propagation. With the exception of one case, a mononuclear cell-predominant vasculitis was present. In some cases the vasculitis was frankly granulomatous. A mononuclear cell dominant vasculitis and neutrophilic vascular reaction pattern co-existed in some cases, recapitulating the dichotomous morphology of virally mediated vascular injury in animal models. In particular, pigs develop granulomatous and neutrophilic vasculitis triggered by porcine reproductive viruses<sup>21</sup>. In one case the intraepithelial pustulation was folliculocentric; interestingly, this case did not demonstrate *in situ* B19 RNA or protein although hepatitis C RNA was detected by *in situ* RT-PCR. Sterile neutrophilic folliculitis with perifollicular vasculopathy is a recently recognized entity that can be associated with systemic diseases such as myeloma or inflammatory bowel disease; however, distant infectious triggers including hepatitis C can trigger an immunologic response that manifests a folliculocentric reaction pattern<sup>20</sup>. The aforesaid vasculopathic changes were typically accompanied by a vacuolar interface dermatitis with foci of interstitial and palisading granulomatous inflammation, a morphologic reaction pattern held to be characteristic of infection-induced reactive arthropathy syndromes<sup>22</sup>.

The localization of viral RNA and protein to endothelium implies a direct role of parvovirus parasitization in the evolution of vasculitis. Globoside, a neutral glycosphingolipid of red cell membranes referred to as the blood group P antigen, is the receptor for B19<sup>23</sup> and is also found in megakaryocytes and endothelial cells<sup>24</sup>. The subsequent events that result in vasculitis likely reflect a combination of direct viral cytotoxicity and humoral immunity. Indeed there was striking morphologic evidence of viral mediated apoptosis and cytolysis, the end point of which was the feulgen-staining, B19-positive basophilic body. The inherent injury mediated by the virus could expose cryptic antigens to which naïve autoreactive T and or B cells react.

Corroborative of a role of true autoimmunity as opposed to a pure nonimmunogenic cytolytic effect was the deposition of C<sub>5b9</sub> within the cutaneous vasculature in 3 cases. Vascular C<sub>5b9</sub> deposition is characteristic of anti-endothelial cell antibody syndromes<sup>25-27</sup>. A similar dual mechanism of vascular injury has been proposed for cytomegalovirus<sup>3</sup>.

The degenerative cellular changes observed in several cases in concert with the localization of viral RNA to the cytolytic cells suggest that virally mediated apoptosis may be a critical mechanism of cellular injury. It has been shown that B19 exerts a cytotoxic effect on infected cells through a non-structural protein it encodes designated NS-1<sup>28</sup>. Specifically, *in vitro* studies have shown that NS-1 induces DNA fragmentation characteristic of apoptosis. Further, the cells infected by B19 are sensitized to TNF- $\alpha$  induced apop-

toxis. Further, the ceramide level is enhanced by B19 infection and NS-1 expression<sup>28</sup>. Ceramide also augments TNF- $\alpha$  mediated apoptosis. Two patients (cases 9 and 15) had periodic fevers accompanied by infiltrative erysipeloid erythema, a symptom complex reminiscent of that seen in the familial periodic fever syndromes in which mutations of the TNF- $\alpha$  receptor complex, perhaps through impaired downregulation of a surface TNF- $\alpha$  receptor and/or diminished shedding of a potentially antagonistic soluble receptor, lead to upregulation of the cytokine cascades during attacks<sup>29-31</sup>.

In summation, the primary finding of this study is that direct endothelial infection by parvovirus was associated with cases of autoimmune disease and vasculitis; most of these patients had a positive serology to B19. Whether this is indicative of a pervasive role of parvovirus in idiopathic CTD awaits further study. Importantly, conventional immunosuppressive therapy was not effective in these patients; one may speculate that this may perpetuate viral infection.

#### ACKNOWLEDGMENT

The authors thank Drs. Peter Schur, Harley Haynes, and Rita Berman, Boston, MA; Bruce Guido, Ashtabula, OH; Kevin Cooper, Leonard Calibrese, Kristen Trotter, and Elizabeth Powers, Cleveland, OH; Richard Narins, Buffalo, NY; Jason Lee, Philadelphia, PA, USA; and Richard Haydey and Martin Karpinski, Winnipeg, MB, Canada for clinical information.

#### REFERENCES

1. Agnello V, Abel G. Localization of hepatitis C virus in cutaneous vasculitic lesions in patients with type II cryoglobulinemia. *Arthritis Rheum* 1997;97:2007-15.
2. Uhoda I, Pierard-Franchimont C, Pierard GE. Varicella-zoster virus vasculitis: a case of recurrent vasculitis without epidermal involvement. *Dermatology* 2000;200:173-5.
3. Golden MP, Hammer SM, Wanke SM, Albrecht MA. Cytomegalovirus vasculitis. Case reports and review of the literature. *Medicine* 1994;73:246-55.
4. Finkel TH, Torok TJ, Ferguson PJ, et al. Chronic parvovirus B19 infection and systemic necrotising vasculitis: opportunistic infection or aetiological agent? *Lancet* 1994;343:1255-8.
5. Nikkari S, Mertsola J, Korvenranta H. Wegener's granulomatosis and parvovirus B19 infection. *Arthritis Rheum* 1994;37:1707-10.
6. Veraldi S, Mancuso R, Rizzitelli G, Gianotti R, Ferrante P. Henoch-Schonlein syndrome associated with human parvovirus B19 primary infection. *Eur J Dermatol* 1999;9:232-3.
7. Fukushige J, Takahashi N, Ueda K, Okada K, Miyazaki C, Maeda Y. Kawasaki disease and human parvovirus B19 antibody: role of immunoglobulin therapy. *Acta Paediatr Jpn* 1995;37:758-60.
8. Staud R, Corman LC. Association of parvovirus B19 infection with giant cell arteritis. *Clin Infect Dis* 1996;22:1123.
9. Magro CM, Dawood MR, Crowson AN. The cutaneous manifestations of human parvovirus B19 infection. *Hum Pathol* 2000;31:488-97.
10. Seidman R, Peress N, Nuovo GJ. In situ detection of PCR-amplified HIV-1 nucleic acids in skeletal muscle in patients with myopathy. *Mod Pathol* 1994;7:369-75.
11. Fridell E, Bekassy AN, Larsson B, Eriksson BM. Polymerase chain reaction with double primer pairs detection of human parvovirus

- B19 induced aplastic crises in family outbreaks. *Scand J Infect Dis* 1992;24:275-82.
12. Nuovo GJ, MacConnell P, French DL. Correlation of the in situ detection of PCR-amplified metalloprotease cDNAs and their inhibitors with prognosis in cervical carcinoma. *Cancer Research* 1995;55:267-75.
  13. Nuovo GJ. PCR in situ hybridization: Protocols and applications. 3rd ed. New York: Lippincott-Raven; 1997.
  14. Lhote F, Guillevin L. Polyarteritis nodosa, microscopic polyangiitis, and Churg Strauss syndrome. Clinical aspects and treatment. *Rheum Dis Clin North Am* 1995;21:911-47.
  15. Nikkari S, Mertsola J, Korvenranta H, Vainionpaa R, Toivanen P. Wegener's granulomatosis and parvovirus B19 infection. *Arthritis Rheum* 1994;37:1707-8.
  16. Diaz, F, Collazos J. Glomerulonephritis and Henoch Schonlein purpura associated with acute parvovirus B19 infection. *Clin Nephrol* 2000;53:237-8.
  17. Watanabe T, Oda Y. Henoch-Schonlein purpura nephritis associated with human parvovirus B19 infections. *Pediatr Int* 2000;42:94-6.
  18. Gabriel SE, Espy M, Erdman DD. The role of parvovirus B19 in the pathogenesis of giant cell arteritis: a preliminary evaluation. *Arthritis Rheum* 2000;42:1255-8.
  19. Bialecki C, Feder HM Jr, Grant-Kels JM. The six classic childhood exanthems: a review and update. *J Am Acad Dermatol* 1989;21:891-903.
  20. Magro CM, Crowson AN. Sterile neutrophilic folliculitis with perifollicular vasculopathy: a distinctive cutaneous reaction pattern reflecting systemic disease. *J Cutan Pathol* 1998;25:215-21.
  21. Thibault S, Drolet R, Germain M. Cutaneous and systemic necrotizing vasculitis in swine. *Vet Pathol* 1998;35:108-16.
  22. Magro CM, Crowson AN. A distinctive cutaneous reaction pattern indicative of infection by reactive arthropathy-associated microbial pathogens: the superantigen ID reaction. *J Cutan Pathol* 1998;25:538-44.
  23. Brown KE, Anderson SM, Young NS. Erythrocyte P antigen: cellular receptor for B19 parvovirus. *Science* 1993;262:114-7.
  24. Cooling LL, Koerner TA, Naides SJ. Multiple glycosphingolipids determine the tissue tropism of parvovirus B19. *J Infect Dis* 1995;172:1198-205.
  25. Crowson AN, Magro CM. The role of microvascular injury in the pathogenesis of cutaneous lesions of dermatomyositis. *Hum Pathol* 1996;27:15-9.
  26. Magro CM, Crowson AN, Regauer S. The dermatopathology of mixed connective tissue disease. *Am J Dermatopathol* 1997; 19:205-12.
  27. Magro CM, Crowson AN. The immunofluorescence findings in cutaneous lesions of dermatomyositis: a comparative study versus lupus erythematosus. *J Cutan Pathol* 1997;24:543-52.
  28. Sol N, Junter JL, Vassias I. Possible interactions between the NS-1 protein and tumor necrosis factor alpha pathways in erythroid cell apoptosis induced by human parvovirus B19. *J Virol* 1999; 73:8762-70.
  29. Schattner A, Lachmi M, Livneh A, Pras M, Hahn T. Tumor necrosis factor in familial Mediterranean fever. *Am J Med* 1991;90:434-8.
  30. McDermott MF, Aksentijevich I, Galon J. Germline mutations in the extracellular domains of the 55 kDa TNF receptor, TNFR1, define a family of dominantly inherited autoinflammatory syndromes. *Cell* 1999;97:133-44.
  31. Gang N, Drenth JP, Langevitz P. Activation of the cytokine network in familial Mediterranean fever. *J Rheumatol* 1999;26:890-7.